



INSTITUT DE FRANCE  
Académie des sciences

# *Comptes Rendus*

---

## *Chimie*

Radia Sennour, Diana Pricop, Nicoleta Platon, Rene Roy  
and Abdelkrim Azzouz

**Optimized diffusion–convection compromise for reversible CO<sub>2</sub> capture  
on hydroxylated organo-montmorillonite**


Volume 25, Special Issue S3 (2022), p. 27-38

Published online: 3 May 2022

<https://doi.org/10.5802/crchim.177>

**Part of Special Issue:** Active site engineering in nanostructured materials for  
energy, health and environment

**Guest editors:** Ioana Fechete (Université de Troyes, France)  
and Doina Lutic (Al. I. Cuza University of Iasi, Romania)

 This article is licensed under the  
CREATIVE COMMONS ATTRIBUTION 4.0 INTERNATIONAL LICENSE.  
<http://creativecommons.org/licenses/by/4.0/>



*Les Comptes Rendus. Chimie sont membres du  
Centre Mersenne pour l'édition scientifique ouverte*  
[www.centre-mersenne.org](http://www.centre-mersenne.org)  
e-ISSN : 1878-1543



---

Active site engineering in nanostructured materials for energy, health and environment /  
*Ingénierie de sites actifs dans les matériaux nanostructurés pour l'énergie, la santé et  
l'environnement*

# Optimized diffusion–convection compromise for reversible CO<sub>2</sub> capture on hydroxylated organo-montmorillonite

Radia Sennour<sup>® a</sup>, Diana Pricop<sup>a</sup>, Nicoleta Platon<sup>® b</sup>, Rene Roy<sup>® a</sup>  
and Abdelkrim Azzouz<sup>® \*, a, c</sup>

<sup>a</sup> Nanoqam, Department of Chemistry, University of Quebec at Montreal,  
QC H3C 3P8, Canada

<sup>b</sup> Catalysis and Microporous Materials Laboratory, Vasile Alecsandri University of  
Bacau, Bacau 600115, Romania

<sup>c</sup> École de Technologie Supérieure, Montréal, QC H3C 1K3, Canada

*E-mails:* sennour.radia@courrier.uqam.ca (R. Sennour),  
pricopdiana2005@yahoo.com (D. Pricop), nicoleta7platon@yahoo.com (N. Platon),  
roy.rene@uqam.ca (R. Roy), azzouz.a@uqam.ca (A. Azzouz)

**Abstract.** Carbon dioxide (CO<sub>2</sub>) was reversibly captured at room temperature and normal pressure by a low cost hybrid absorbent (NaMt-H30) obtained through Na-montmorillonite intercalation with Boltorn dendrimer H30 (1 wt%). Measurements through thermal programmed desorption between 20 °C and 200 °C showed variations of the retention capacities of CO<sub>2</sub> (CRC) and water (WRC) according to the nitrogen stream throughput, contact time and injected CO<sub>2</sub> amount for adsorbent saturation. CRC and WRC modeling as functions of these parameters was achieved using a 3<sup>3</sup> factorial design involving 27 attempts. Model analysis revealed that the retention of CO<sub>2</sub> and water molecules depend not only on the individual effects of each parameters but also on their interactions. High nitrogen throughput and low amount of impregnation resulted in detrimental effects on both CO<sub>2</sub> and moisture retention. This was explained in terms of diffusion and mass loss during impregnation through forced convection. An optimum compromise between these factors in correlation with the contribution of moisture content turned out to be an essential requirement for achieving highest CRC levels that express the effective material affinity towards carbon dioxide. These findings provide a useful tool for rigorously optimizing the reversible capture of CO<sub>2</sub> by hydroxylated adsorbents.

**Keywords.** Reversible capture, Carbon dioxide, Polyol dendrimers, Montmorillonite, Optimization.

*Published online:* 3 May 2022

---

\* Corresponding author.

## 1. Introduction

Carbon dioxide (CO<sub>2</sub>) is regarded as one of the main factors of the greenhouse gas effect and eventual global warming [1,2]. Since CO<sub>2</sub> production is difficult to be suppressed or diminished, reduction of CO<sub>2</sub> emissions at the very emission source has become a major issue to be addressed. Gas capture methods using compounds like amines, white-wash or base-like adsorbents such as alkaline ash, activated carbons, porous silica, zeolites, ions exchange resins and mesoporous silicates, activated alumina, metal oxide and others showed promising prospects [3,4].

However, such methods unavoidably produce wastes like carbamates and carbonates that need to be removed or regenerated. So-called Temperature Swing Adsorption (TSA) and Pressure Swing Adsorption (PSA) techniques for on-site regeneration via repetitive fluctuations of temperature and pressure without removing the adsorbents showed satisfactory performances in treating industrial flue emissions [5–7]. However, their energy consumption even partly compensated by the heat evacuated by the very flue emission, the use of organic compounds and production of undesirable by-products still remain major shortcomings.

The reversible capture of CO<sub>2</sub> at ambient temperature from low concentrated gas emissions requires a new approach that targets gas retention in CO<sub>2</sub>-rich atmospheres with subsequent release at nearly ambient conditions in less concentrated media. This concept involves respiratory systems for concentrating CO<sub>2</sub> onto a solid surface that can be regenerated by a mere equilibrium contact with CO<sub>2</sub>-free media or upon forced convection under strong carrier gas stream. This concept has barely been tackled so far. The targeted equilibrium shift that favors CO<sub>2</sub> desorption requires not only specific adsorption sites capable of displaying weak and purely physical interactions with CO<sub>2</sub> on the adsorbent surface but also optimization of many parameters that govern these interactions.

Successful attempts in this regard have demonstrated that CO<sub>2</sub> can reversibly be retained through weak interaction with amphoteric to weakly basic surfaces. Indeed, CO<sub>2</sub> was found to adsorb on a wide variety of clay-supported polyalcohols. The OH groups of the incorporated organic moieties were

found to act as adsorption sites [8–11]. The moisture content of such adsorbents showed a significant contribution to CO<sub>2</sub> retention [9,12]. One of these organoclay materials, namely montmorillonite intercalated with H30 Bolton dendrimer has particularly attracted attention. Due to its optimum surface properties, appreciable CO<sub>2</sub> retention capacity (CRC) was induced by increased number of available OH groups without intermolecular dendrimer aggregation into dense hydrophobic clusters [11–13].

The adsorption–desorption cycle on OH-enriched montmorillonites appears to be strongly influenced by a series of parameters such as temperature, total pressure, CO<sub>2</sub> partial pressure, contact time and carrier gas throughput [9,12,13]. The lack of data dealing with the effects and possible interactions occurring between these parameters has stimulated research in this direction. For this purpose, the reversible capture of CO<sub>2</sub> was modeled and optimized using 3<sup>3</sup> factorial experiment designs. Preliminary experiments showed that, as expected, numerous factors can influence the adsorption desorption of CO<sub>2</sub>, but only some of them, namely the flow rate, contact time and impregnating CO<sub>2</sub> quantity can be regarded as being key parameters that govern the processes efficiency. A judicious choice of the parameters range is an essential requirement for achieving high CRC values. The latter along with the water moisture were modeled as response-functions using Na<sup>+</sup> exchanged montmorillonite containing 1 wt% of dendrimer H30 (NaMt-H30). The individual effects and interactions of these parameters were investigated in order to detect and assess a possible synergy on CO<sub>2</sub> adsorption.

## 2. Materials and methods

### 2.1. Preparation of NaMt-H30 and characterization

Na<sup>+</sup> exchanged montmorillonite (NaMt) containing 1 wt% of dendrimer H30 (NaMt-H30) has been prepared and characterized in previous works [9,11–13]. As a reminder, NaMt originated from the purification of commercial crude bentonite supplied by Aldrich with a 1.58 silica/alumina weight ratio, as previously described. A bulky polyester-alcohol with the chemical formula 2,2-bis(methylol)propionic acid (bis-MPA) with an idealized structure illustrated in

Scheme 1 was employed as organic moiety [14,15]. This compound is commercially designated as dendrimer H30 (supplied by Boltorn Technology Co. Ltd.) and having an average  $3607.6 \text{ g}\cdot\text{mol}^{-1}$  molecular weight.

Clay intercalation with H30 was achieved by mere electrostatic self-assembly in aqueous media between a NaMt suspension and the organic polyol species. For this purpose, attempts were performed by impregnating NaMt samples in powder form (500 mg) with a diluted aqueous solution containing 1 wt% polyol H30 (5 mg). The resulting mixture was then stirred overnight at room temperature. The organoclay sample (organo-Mt) was dried overnight at room temperature until total evaporation of the solvent, and then at  $120 \text{ }^\circ\text{C}$  for 6 h before being smoothly crushed for preventing structure alteration.

NaMt and NaMt-H30 were both characterized by X-rays diffraction (Siemens D5000 instrument, Co-K $\alpha$  at  $1.7890 \text{ \AA}$ ), Fourier Transform infrared ATR-mode spectroscopy (using a KBr IR cell and a Model IR 550 Magna Nicolet instrument) and thermal gravimetric analyses (TG/TDA6200 Seiko Instrument Inc., under a  $100 \text{ mL}\cdot\text{min}^{-1}$  nitrogen stream and a  $5 \text{ }^\circ\text{C}\cdot\text{min}^{-1}$  heating rate) [9,11–13]. The specific surface area and pore size distribution were assessed by BET method calculations. For this purpose, measurements through  $\text{N}_2$  adsorption isotherms were achieved at 77 K by means of a Quantachrome Instruments equipped with an Autosorb automated gas sorption system control. For the sake of conciseness, the related spectra and diagrams are not shown in this work, but their results were only discussed herein in correlation with the adsorptive properties.

## 2.2. Thermal programmed desorption

The retention strength and  $\text{CO}_2$ /water retention capacities (CRC and WRC, respectively) were assessed through thermal programmed desorption (TPD). The retention strength was regarded as being proportional to the desorption temperature (desorption peak), while the CRC was defined as the area described by the TPD pattern and expressed in terms of micromole  $\text{CO}_2$  desorbed per gram of dry clay material between  $20 \text{ }^\circ\text{C}$  and  $200 \text{ }^\circ\text{C}$ . This upper temperature limit was determined by TG-DTG measurements, which revealed a thermal stability thresh-

old of up to  $240 \text{ }^\circ\text{C}$  for NaMt-H30. Preliminary investigations showed that optimum amount (50 mg) and particle size (0.01–0.1 mm) of the adsorbent sample allowed preventing diffusion phenomenon during TPD runs under nitrogen stream not exceeding  $15 \text{ mL}\cdot\text{min}^{-1}$ . Prior to TPD measurements, each sample was dried in a 10 mm tubular glass reactor under a  $15 \text{ mL}\cdot\text{min}^{-1}$  dry nitrogen stream at  $160 \text{ }^\circ\text{C}$  for 1 h, and then cooled to  $20 \text{ }^\circ\text{C}$ . At this temperature,  $\text{CO}_2$  was injected without nitrogen (static mode) for accurate CRC assessment. After saturation, the non-adsorbed  $\text{CO}_2$  excess was evacuated by the nitrogen stream at the throughput selected for TPD until no  $\text{CO}_2$  is detected by Li-840A  $\text{CO}_2/\text{H}_2\text{O}$  Gas Analyzer (Li-COR Bioscience Inc., USA) at the TPD device outlet after 40–60 min. TPD measurements were performed between  $20 \text{ }^\circ\text{C}$  and  $200 \text{ }^\circ\text{C}$  at a heating rate of  $5 \text{ }^\circ\text{C}\cdot\text{min}^{-1}$  under  $1\text{--}5 \text{ mL}\cdot\text{min}^{-1}$  nitrogen stream. Here, care should be taken in CRC measurements, because higher nitrogen flow rates during saturation were found to remove the adsorbed  $\text{CO}_2$  by mere convection even without heating.

## 2.3. Adsorption capacity modeling

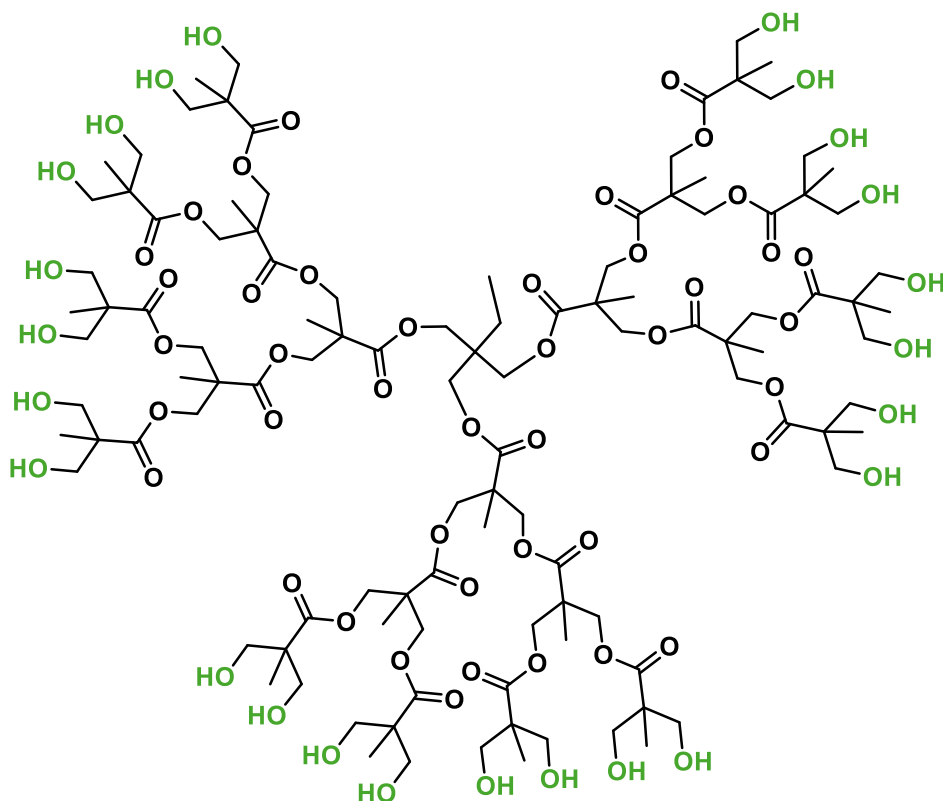
Thus, 27  $\text{CO}_2$  adsorption attempts were made according to a  $3^3$  experiment factorial design, by varying the nitrogen flow rate from 1 to  $15 \text{ }^\circ\text{C}\cdot\text{min}^{-1}$  ( $X_1$ ), contact time from 1 to 12 hours ( $X_2$ ) and quantity of carbon dioxide from 1 to 6 mmol ( $X_3$ ) in suitable parameters ranges (Table 1).

The model calculations were achieved using non-dimensional or reduced values of these parameters and each parameter was varied on three levels, i.e., (i)  $-1$  for the minimum value, (ii)  $0$  for the medium value, and (iii)  $+1$  for the maximum value of the respective parameter. The CRC and WRC were considered as optimality criteria for each of the 27 different attempts.

## 3. Results and discussion

### 3.1. Structure of NaMt-H30

The structure of NaMt-H30 had been richly investigated in our previous papers [9,11–13,16]. The powder XRD data indicated the transition from a random to a face-to-face parallel layout of the clay sheets and an optimum ratio of 1 wt% H30 for an enlargement



**Scheme 1.** Idealized configuration of Boltorn dendrimer H30.

of the interlayer spacing without altering the ordered layout of the clay lamellae. The influence of the OH groups from the clay on the incorporated dendrimer was also detailed in our previous work [10–13,16–18]. The uniform H30 spread in the clay surface produced only a slight improvement of the specific surface area from  $45\text{--}50\text{ m}^2\cdot\text{g}^{-1}$  to  $54\text{ m}^2\cdot\text{g}^{-1}$ , presumably due to slight structure compaction induced by interactions between next-neighboring organoclay lamellae [11,19].

### 3.2. Moisture contribution to $\text{CO}_2$ capture

The surface basicity and hydrophilic character expressed in terms of CRC and WRC were the main features investigated herein. Given the higher thermal stability of unmodified NaMt up to  $550\text{ }^\circ\text{C}$ , repetitive  $\text{CO}_2$ -TPD attempts ( $\text{CO}_2$ -TPD1 to  $\text{CO}_2$ -TPD3) without alternate rehydration after each TPD cycle

were run between  $20\text{ }^\circ\text{C}$  and  $450\text{ }^\circ\text{C}$ . The results obtained revealed significant changes in the TPD profiles for both  $\text{CO}_2$  and water (Figure 1). The significant CRC decay observed between  $220\text{ }^\circ\text{C}$  and  $450\text{ }^\circ\text{C}$  accounts for an advanced removal of medium and strong basicities. Indeed, three successive thermal desorption-cooling-dry  $\text{CO}_2$  re-injection cycles induced a marked CRC decay for  $\text{CO}_2$ -TPD2 after TPD1 even more pronounced for  $\text{CO}_2$ -TPD3 after TPD2. Simultaneously, a marked depletion of the hydrophilic character for  $\text{H}_2\text{O}$ -TPD2 even more accentuated for  $\text{H}_2\text{O}$ -TPD3 took place, as reflected by visible CRC decreases in the WRC (Figure 1b).

It is worth mentioning that repetitive TPD runs after alternate rehydration by injecting moisture saturated  $\text{CO}_2$  resulted in TPD patterns (TPD-R) perfectly similar to that of TPD1 for both  $\text{CO}_2$  and water. This result is of great importance, because it confirms the thermal stability of the starting clay mineral at least up to  $450\text{ }^\circ\text{C}$ . It is clear that below this thermal stabil-

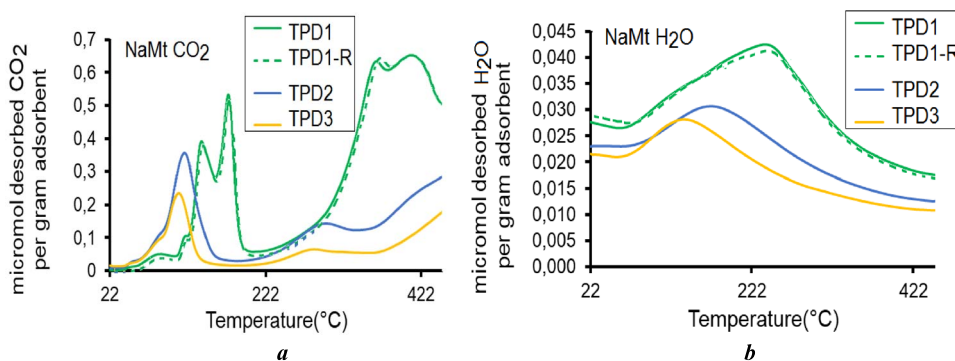


**Figure 1.** Repetitive TPD patterns for CO<sub>2</sub> (a) and water (b) under 15 mL·min<sup>-1</sup> nitrogen stream. TPD1, TPD2 and TPD3 were recorded after repetitive CO<sub>2</sub>-adsorption-thermodesorption cycles with rehydration. TPD1 and TPD1-R were recorded after repetitive CO<sub>2</sub>-adsorption-thermodesorption cycle with alternate rehydration by injecting moisture saturated CO<sub>2</sub>.

**Table 1.** Parameter levels and ranges for 3<sup>3</sup> factorial design at  $T = 25$  °C

| Parameter level                                  |        | Minimum | Medium | Maximum |
|--|--------|---------|--------|---------|
| Coded value (non-dimensional)                    | Symbol | -1      | 0      | +1      |
| Nitrogen throughput (mL·min <sup>-1</sup> )      | $X_1$  | 1       | 8      | 15      |
| Contact time (h)                                 | $X_2$  | 1       | 6.5    | 12      |
| Injected CO <sub>2</sub> (mmol·g <sup>-1</sup> ) | $X_3$  | 20      | 70     | 120     |

ity threshold, NaMt rehydration revives the CRC and that water also contributes to CO<sub>2</sub> capture.

### 3.3. Adsorptive properties of NaMt-H30

NaMt-H30 exhibited appreciable thermal stability, barring dehydration between 80 °C and 140 °C, no degradation of the organic moiety was detected up to 240 °C. Such a thermal stability allowed establishing the temperature range for TPD measurements between 20 °C and 200 °C with high accuracy. TPD measurements were achieved for the 27 attempts involved in the factorial 3<sup>3</sup> experiment design, by varying three key parameters, namely the carrier gas flow-rate ( $X_1$ ), contact time ( $X_2$ ) and impregnating CO<sub>2</sub> quantity ( $X_3$ ). The CRC, expressed in terms of desorbed CO<sub>2</sub> amount in the investigated temperature range, showed values in the range 34.4–609.1  $\mu\text{mol}\cdot\text{g}^{-1}$  for nitrogen throughputs of 1–15 mL·min<sup>-1</sup> (Table 2).

Preliminary observations showed that lowest flow rates, medium saturation time and medium to high amount of injected CO<sub>2</sub> gave the highest CRC values (441.3–609.2  $\mu\text{mol}\cdot\text{g}^{-1}$ ). Conversely, high carrier gas throughput resulted in lowest CRC levels (34.4–53.1  $\mu\text{mol}\cdot\text{g}^{-1}$ ), thereby confirming CO<sub>2</sub> capture via weak interaction with the OH groups of the organoclay and easy release upon forced convection without heating. The high discrepancy between the highest and lowest CRC levels accounts for 64–94.4% of the nominal CRC value obtained in these experiments. This result is of great importance, because it clearly demonstrates the occurrence of truly reversible capture of CO<sub>2</sub>, and that forced convection affects CRC assessments.

### 3.4. Model calculations and accuracy

CO<sub>2</sub> retention capacity (CRC) values and water retention capacity (WRC) values were modeled on the basis of the 27 experimental attempts, using a Taylor's second-order polynomial model [20–23]. Before

**Table 2.** 3<sup>3</sup> Parameter combinations and corresponding two response-functions as optimality criteria

| Key-parameters levels (Non-dimensional units) |                                 |   | Response function = Retention capacity ( $\mu\text{mol}\cdot\text{g}^{-1}$ ) |  |                                      |  |
|---|---------------------------------|---|--|--|--------------------------------------|--|
| Flow $X_1$                                    | Contact time <sup>a</sup> $X_2$ | CO <sub>2</sub> amount <sup>b</sup> $X_3$ | CRC  | WRC                                      |                                      |  |
| -1  | -1                              | -1  | 386.6  | 1.06                                     |                                      |  |
|   |                                 | 0   | 385.4  | 1.06                                     |                                      |  |
|   |                                 | 1   | 254.6  | 0.44                                     |                                      |  |
|   | 0                               | -1  | -1   | 350.3                                    | 3.81                                 |  |
|   |                                 |   | 0  | 441.3                                    | 2.98                                 |  |
|   |                                 |   | 1  | 609.1                                    | 2.90                                 |  |
|   | 1                               | -1  | -1   | 279.8                                    | 3.24                                 |  |
|   |                                 |   | 0  | 304                                      | 3.18                                 |  |
|   |                                 |   | 1  | 366.6                                    | 4.18                                 |  |
| 0   | -1                              | -1  | 65.7   | 0.64                                     |                                      |  |
|   |                                 | 0   | 81.7   | 0.24                                     |                                      |  |
|   |                                 | 1   | 73.4   | 0.29                                     |                                      |  |
|   | 0                               | -1  | -1   | 39.3                                     | 0.61                                 |  |
|   |                                 |   | 0  | 141.2 <sup>c</sup> (143.0; 140.5; 140.0) | 1.38 <sup>c</sup> (1.39; 1.35; 1.50) |  |
|   |                                 |   | 1  | 169.2                                    | 3.93                                 |  |
|   | 1                               | -1  | -1   | 48.9                                     | 0.82                                 |  |
|   |                                 |   | 0  | 153.5                                    | 1.59                                 |  |
|   |                                 |   | 1  | 185.8                                    | 1.82                                 |  |
| 1   | -1                              | -1  | 53.1   | 0.24                                     |                                      |  |
|   |                                 | 0   | 51.2   | 0.18                                     |                                      |  |
|   |                                 | 1   | 49.4   | 0.27                                     |                                      |  |
|   | 0                               | -1  | -1   | 49.3                                     | 1.03                                 |  |
|   |                                 |   | 0  | 93.4                                     | 1.02                                 |  |
|   |                                 |   | 1  | 111.1                                    | 0.89                                 |  |
|   | 1                               | -1  | -1   | 44.2                                     | 1.19                                 |  |
|   |                                 |   | 0  | 35.3                                     | 2.10                                 |  |
|   |                                 |   | 1  | 34.4                                     | 1.24                                 |  |

<sup>a</sup> The contact time accounts for the saturation time imposed for the sample impregnation with a given CO<sub>2</sub> amount.

<sup>b</sup> The CO<sub>2</sub> amount is the injected quantity to be contacted with the dry powder sample for impregnation up to saturation prior to TPD run.

<sup>c</sup> The average CRC and WRC values for the (0, 0, 0) experiment were assessed by calculation the mean of the three measurements registered at this experimental point and are given herein between brackets. All CRC and WRC values were calculated on the basis of TPD measurements in the range 20–200 °C.

model refinement, the general Taylor equation for both the CRC and WRC (denoted as  $Y$ ) is given by (1):

$$Y = a_0 + a_1 \cdot X_1 + a_2 \cdot X_2 + a_3 \cdot X_3 + a_{11} \cdot X_1^2 + a_{22} \cdot X_2^2 + a_{33} \cdot X_3^2 + a_{12} \cdot X_1 \cdot X_2 + a_{13} \cdot X_1 \cdot X_3 + a_{23} \cdot X_2 \cdot X_3 + a_{123} \cdot X_1 \cdot X_2 \cdot X_3. \quad (1)$$

The calculations of the model coefficients are not described in the present work, but details about the method used are described elsewhere [21]. The calculated values of the model coefficients (Table 3) are assumed to describe the individual effects of the investigated parameters and their possible interactions. The model adequacy strongly depends on the accuracy of the experiment measurements, where the main errors arise from volume and weight measurements. For this purpose, three additional attempts at the central point (0,0,0) are required for estimating the average error in calculating the value of each coefficient on the basis of the random variance (Table 4).

Model refining using the  $t$ -student test gave lower average error of 0.133 than the very coefficient values. Therefore, all coefficients were maintained in the CRC model (2). Application of the same Student's  $t$  test to the WRC model gave higher  $|\Delta a_i|$  (0.332) than coefficients  $a_3$ ,  $a_{33}$ ,  $a_{13}$ ,  $a_{23}$  and  $a_{123}$ . Removing these coefficients were removed from the WRC model (3) suggests negligible effect and interactions of their common parameter, namely the injected CO<sub>2</sub> amount ( $X_3$ ) on the moisture content.

$$\begin{aligned} \text{CRC} = & 156.8 - 158.7 \cdot X_1 + 2.86 \cdot X_2 + 29.8 \cdot X_3 \\ & + 110.1 \cdot X_1^2 - 64.2 \cdot X_2^2 - 11.4 \cdot X_3^2 \\ & + 3.0 \cdot X_1 \cdot X_2 - 13.8 \cdot X_1 \cdot X_3 \\ & + 28.5 \cdot X_2 \cdot X_3 - 28.1 \cdot X_1 \cdot X_2 \cdot X_3 \end{aligned} \quad (2)$$

$$\begin{aligned} \text{WRC} = & 1.709 - 0.82 \cdot X_1 + 0.83 \cdot X_2 + 0.18 \cdot X_3 \\ & + 0.47 \cdot X_1^2 - 0.74 \cdot X_2^2 \\ & + 0.06 \cdot X_3^2 - 0.35 \cdot X_1 \cdot X_2 \\ & + 0.05 \cdot X_1 \cdot X_3 + 0.25 \cdot X_2 \cdot X_3 \\ & - 0.19 \cdot X_1 \cdot X_2 \cdot X_3. \end{aligned} \quad (3)$$

A method of adequacy test was achieved through the Fisher's test, expressed in terms of the quotient of the random variance, previously calculated and the residual variance estimated in Table 4. In this case also, both calculated models (with 3 degrees of freedom) are considered to fit the CRC and WRC in the same range, because  $F \gg F_{0.95,3,4}$  with a 95% confidence.

### 3.5. Effect simulation and optimization

The individual effects and interactions of the parameters were discussed on the basis of the sign and the absolute value of each coefficient. These coefficient features will define the direction and intensity of the corresponding effect (favorable or detrimental) on CRC and WRC assessment. As expected, the carrier gas throughput displayed the strongest detrimental effect on the CRC and to a lesser extent on the WRC, confirming once again that both CO<sub>2</sub> and water are weakly retained and that the occurrence of forced convection affects the assessment both retention capacities.

As a general tendency, increasing nitrogen throughput reduces the CRC. However, increasing contact time during adsorption induced a much weaker influence on the CRC but a favorable individual effect on the WRC. This must be due to stronger diffusion hindrance of non-linear and more polar water molecules within the organoclay entanglement as compared to CO<sub>2</sub>.

The values of the quadratic coefficients,  $a_{ii}$ , are essential criteria for estimating the concavity (convexity) of the response surface. The opposite signs of the quadratic coefficients and concavity decrease in the following sequence:  $|a_{11}| \gg |a_{22}| > |a_{33}|$ , allowed predicting a pronounced minimum of the CRC response-surface with respect to the nitrogen throughput and flattened maximum with respect to the contact time (Figure 2a). A similar but more flattened saddle-shaped response-surface was observed when replacing the contact time ( $X_1$ ) by the injected CO<sub>2</sub> ( $X_3$ ) (Figure 2b). This confirms the strong influences of the investigated parameters.

Informative plots were obtained for CRC =  $f(X_2, X_3)$  with  $X_1 = 0$  or 1 (Figure 3). The obtained response-surface revealed CRC maxima at optimum values of the contact time ( $X_2$ ) and impregnating CO<sub>2</sub> amounts ( $X_3$ ). The occurrence of optimum contact time must be due to slow gas diffusion with the organoclay dendritic entanglement. The fact that the optima are included within the investigated parameters ranges provides clear confirmation of the model validity. Analytical resolution of the equation system resulting from the first derivation of the CRC models for  $X_1 = 0$  gave optimum values of  $X_2 = 0.438$  and  $X_3$  outside the investigated parameter range (1.872).



**Table 3.** Model coefficients and simulated effects upon CRC and WRC assessment

| Model coefficient | Parameter effect on CRC assessment |  | Parameter effect on WRC assessment |                               |
|-------------------|------------------------------------|--|------------------------------------|-------------------------------|
|                   | Value                              | Simulated effect                             | Value                              | Simulated effect              |
| $a_0$             | 156.8                              | Dummy variable                               | 1.709                              | Dummy variable                |
| $a_1$             | -158.7                             | Strongly detrimental individual effect       | -0.816                             | Detrimental individual effect |
| $a_2$             | 2.86                               | Weakly favorable individual effect           | 0.829                              | Favorable individual effect   |
| $a_3$             | 29.80                              | Favorable individual effect                  | 0.184*                             | Removed from the model        |
| $a_{12}$          | 3.03                               | Weakly favorable $X_1$ - $X_2$ interaction   | -0.350                             | Minimum according to $X_1$    |
| $a_{13}$          | -13.78                             | Weakly detrimental $X_1$ - $X_3$ interaction | 0.045*                             | Removed from the model        |
| $a_{23}$          | 28.49                              | Favorable $X_2$ - $X_3$ interaction          | 0.245*                             | Removed from the model        |
| $a_{11}$          | 110.09                             | Sharp minimum according to $X_1$             | 0.465                              | Minimum according to $X_1$    |
| $a_{22}$          | -64.16                             | Maximum according to $X_2$                   | -0.740                             | Maximum according to $X_2$    |
| $a_{33}$          | -11.29                             | Flattened Maximum according to $X_3$         | 0.062*                             | Removed from the model        |
| $a_{123}$         | -28.11                             | Detrimental ternary interaction              | -0.194                             | Removed from the model        |

\* These coefficients are smaller than the average error on their values (trust range).

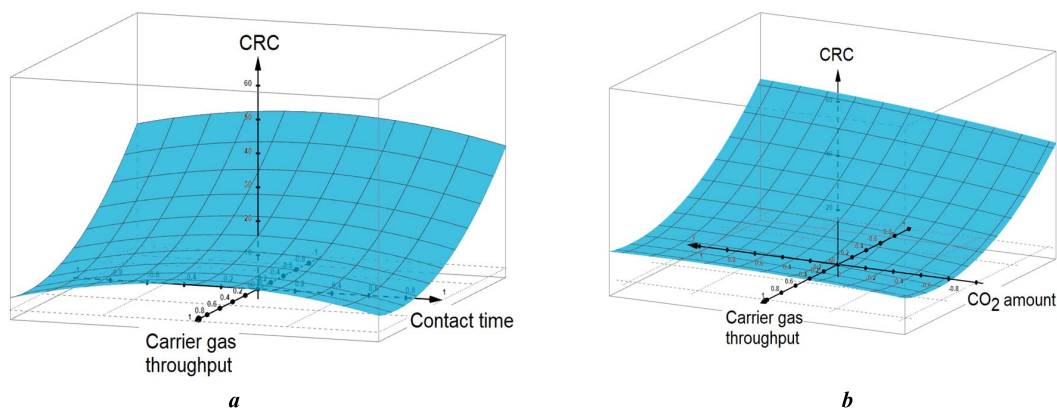


**Figure 2.** 3D plot of CRC as a function of non-dimensional values of  $X_1$  and  $X_2$  for  $X_3 = 0$  (a) and of  $X_1$  and  $X_3$  for  $X_2 = 0$  (b) for centered values of the non-plotted parameters.  $X_1$ : carrier gas throughput;  $X_2$ : contact time;  $X_3$ : Injected  $\text{CO}_2$  amount.

Similar calculations for  $X_1 = 1$  gave optimum  $X_2 = 0.048$  and  $X_3 = 0.71$ . As expected, calculations using these values in the CRC model gave values below  $20 \mu\text{mol}\cdot\text{g}^{-1}$  for highest and medium carrier gas throughputs (+1 and 0). This can be explained by the occurrence of forced convection that can release both  $\text{CO}_2$  and water molecules, in agreement with our previous statements. This suggests that other optimum parameters should occur at the lowest carrier gas throughput. The

shape of CRC plot for the slowest throughput of the carrier gas ( $X_1 = -1$ ) allowed predicting a clear optimum (Figure 4). Calculations using the corresponding CRC model resulted in values included within the investigated parameters ranges ( $X_2 = 0.40$  and  $X_3 = 0.92$ ). Conversion of these non-dimensional values gave optimum contact time ( $X_2$ ) of 8.7 h and amount of impregnating  $\text{CO}_2$  ( $X_3$ ) of  $24.1 \text{ mmol}\cdot\text{g}^{-1}$ . Qualitative CRC assessment using these optimum parameters in the model re-

**Table 4.** Model adequacy tests at (0,0,0) point and variance analysis for CRC and WRC assessments

| Feature                                | Symbol/Equation  | Model adequacy                   |                                    |
|--|--|----------------------------------|------------------------------------|
|  |  | CRC                              | WRC                                |
| Parameter number                       | $P$  | 3                                | 3                                  |
| Level number                           | $L$  | 3                                | 3                                  |
| Experimental attempt number            | $N$  | 27                               | 27                                 |
| Attempt number at (0,0,0) point        | $n$  | 3                                | 3                                  |
| Model variance                         | $v$  | 2                                | 2                                  |
| Retention capacity at (0,0,0) point    | $y_{01}$   | 143.0                            | 1.00                               |
|  | $y_{02}$   | 140.5                            | 1.35                               |
|  | $y_{03}$   | 140.1                            | 1.80                               |
| Mean at (0,0,0) point                  | $y_0 = \sum y_{0i} / 3$                                  | 141.17                           | 1.38                               |
| Random variance                        |  | 2.583                            | 0.16                               |
| Square root of variance                | $S$  | 1.607                            | 0.40                               |
| Risk factor                            | $\alpha^*$   | 0.05                             | 0.05                               |
| Student's $t$ test factor              | $t_{v,1-\alpha/2}$                                       | 4.3 <sup>b</sup>                 | 4.3 <sup>b</sup>                   |
| Average error on the coefficient value | $\Delta_{a_i} = \pm t_{v,1-\alpha/2} \times (S/N)^{0.5}$ | $\pm 1.33$                       | $\pm 0.332$                        |
| Coefficients to be eliminated          | $ a_i  <  \Delta_{a_i} $ (Student's $t$ test)            | None                             | $a_3, a_{13}, a_{23}$ and $a_{33}$ |
| Number of remaining coefficients       | $R$  | 11                               | 7                                  |
| Model response at (0,0,0)              | $y(0,0,0) = a_0$   | 157.0                            | 1.709                              |
| Average yield for the 27 attempts      | $Y_m = \sum Y_i / 27$                                    | 179.9                            | 1.567                              |
| Residual variance                      | $S_r^2 = \sum (Y_i - Y_m)^2 / (N - R)$                   | 40,314                           | 2.058                              |
| Fisher's test (Fisher–Snedecor law)    | Second test for model adequacy $F = Sr^2 / S^2$          | 15,606 ><br>$F_{0.95,3,4} = 6.6$ | 12.79 ><br>$F_{0.95,3,4} = 6.6$    |

Risk factor:  $\alpha = 0.05$  was arbitrary chosen. In this case, a 95% confidence was regarded as being satisfactory.

$t_{2,0.95} = 4.3$  (Student Law with 2 degrees of freedom at a 95% confidence).

$F_{0.95,3,4} = 6.6$  (see Fisher–Snedecor tables). To invalidate the hypothesis that all the coefficients of the model are equal to zero or to validate that at least one coefficient is different from zero, the calculated  $F$ -test should be higher than the theoretical value of 6.6 provided by the tables.

sulted in the highest CRC of 35  $\mu\text{mol}\cdot\text{g}^{-1}$  among those calculated for various parameter combinations. This CRC is much lower than those obtained by additional triplicate experiments (65.0, 59.4 and 68.2  $\mu\text{mol}\cdot\text{g}^{-1}$ ) under the above determined optimum parameters.

This result confirms once again that the CRC cannot be accurately assessed using such a mathematical model, which is rather intended for parameter optimization. An attempt justified by economic reasons, achieved for minimum contact time ( $X_2 = -1$ ) failed because of even lower estimated CRC values, below 10  $\mu\text{mol}\cdot\text{g}^{-1}$ . Thus, it is clear that unlike slow

gas stream for avoiding forced convection, minimum contact time cannot be an essential requirement for achieving effective  $\text{CO}_2$  capture on NaMt-H30. Here, the unavoidable diffusion hindrance imposes sufficiently long contact times of such adsorbents, but is not necessarily a major drawback being compensated by the non-stoichiometric capture of  $\text{CO}_2$ . Indeed, a 50 mg NaMt-H30 sample with a 1 wt% polyol H30 ( $M = 3607.6 \text{ g}\cdot\text{mol}^{-1}$  and 32 OH/mole) accounts for 88.7  $\mu\text{moles}$  OH per gram adsorbent.

This is by far lower than the highest CRC value determined in the  $3^3$  factorial design (609.1  $\mu\text{mol}\cdot\text{g}^{-1}$ ) (Table 2) and those obtained by additional tripli-

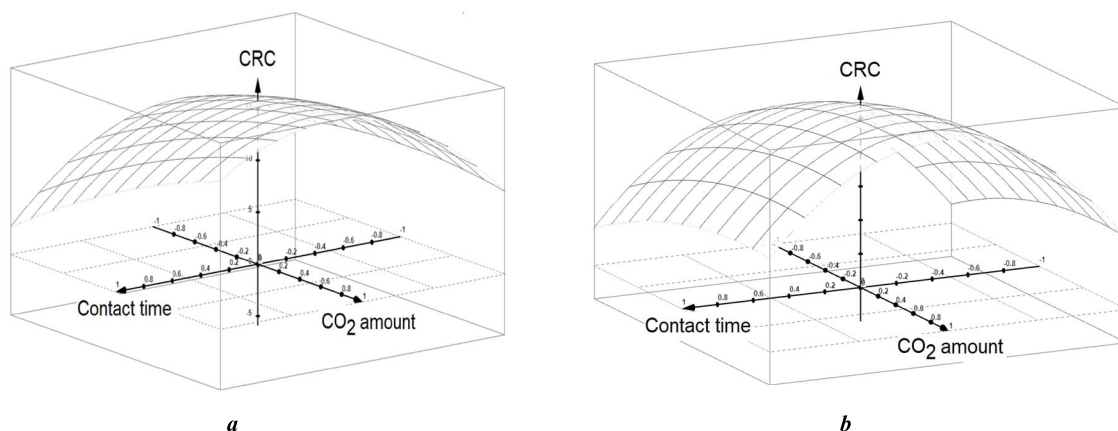


**Figure 3.** 3D CRC plot as a function of non-dimensional values of  $X_2$  and  $X_3$  for  $X_1 = 0$  (a) and for  $X_1 = 1$  (b).  $X_1$ : carrier gas throughput;  $X_2$ : contact time;  $X_3$ : Injected  $\text{CO}_2$  amount.

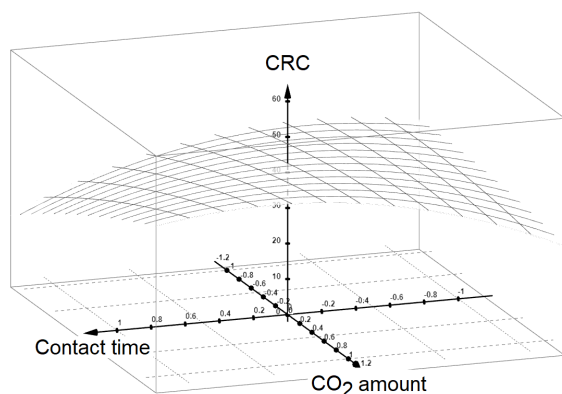


**Figure 4.** 3D CRC plot as a function of non-dimensional values of  $X_2$  and  $X_3$  for minimum value of the carrier gas throughput ( $X_1 = -1$ ).  $X_1$ : carrier gas throughput;  $X_2$ : contact time;  $X_3$ : Injected  $\text{CO}_2$  amount.

cate experiments ( $650.0$ ,  $594.0$  and  $682.0 \mu\text{mol}\cdot\text{g}^{-1}$ ). It results that each OH group in NaMt-H30 can retain more than 13  $\text{CO}_2$  molecules. This is a significant result that allows envisaging even higher effectiveness by increasing the number of available OH groups. This can be achieved through higher polyol dendrimer dispersion of the clay surface for minimizing the intermolecular H-bridges. The surprising occurrence of an optimum contact time for the

CRC can only be explained a similar phenomenon for the WRC for both medium and slow carrier gas throughput (Figure 5).

Insufficient contact time is assumed to affect the moisture content due to slow water molecule diffusion in agreement with previous statements. Conversely, long contact time should probably favor the diffusion of linear  $\text{CO}_2$  at the expense of bulkier water molecules. The resulting decrease in moisture content is expected to reduce water- $\text{CO}_2$  interaction and subsequently the CRC. This result is of great importance, because it clearly confirms the narrow interaction between the surface basicity and hydrophilic character in such OH-enriched organoclays.

#### 4. Conclusion

Montmorillonite intercalation by dendrimer Boltorn H30 induced an improvement in the affinity towards both moisture and carbon dioxide, with favorable reciprocal interaction between both compounds. The polynomial models describing the capacities for carbon dioxide and water retention showed strong interaction between both adsorbed  $\text{CO}_2$  and water molecules. Their retention depends on parameter effects and interactions. High nitrogen throughput and low amount of impregnating  $\text{CO}_2$  induce

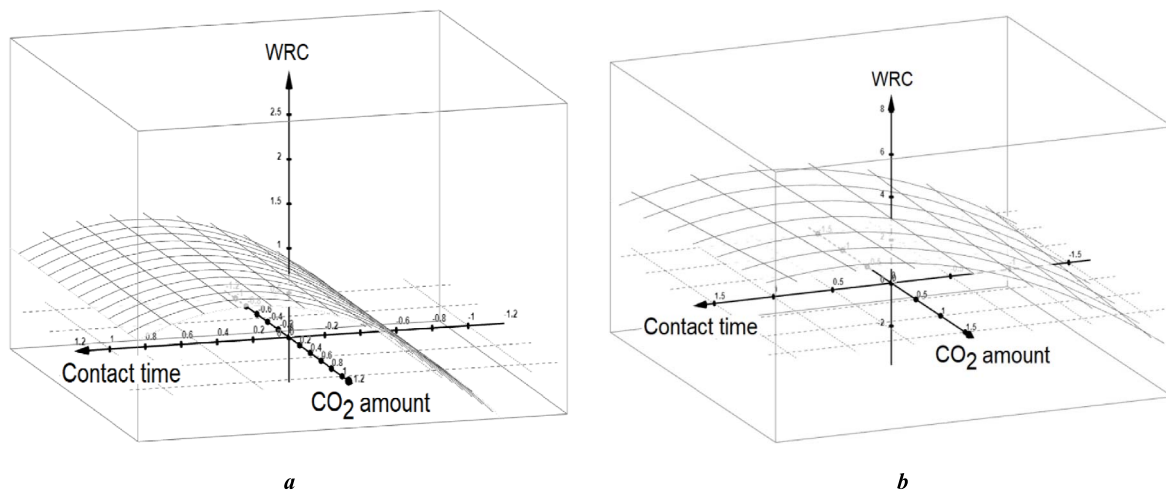


**Figure 5.** 3D WRC plot as a function of non-dimensional values of  $X_2$  and  $X_3$  for  $X_1 = 0$  (a) and  $X_1 = -1$  (b).  $X_1$ : carrier gas throughput;  $X_2$ : contact time;  $X_3$ : Injected  $\text{CO}_2$  amount.

detrimental diffusion hindrance and mass loss during impregnation through forced convection. Effective  $\text{CO}_2$  capture requires an optimum compromise between these factors and the moisture content. These results provide a useful tool for envisaging the reversible capture of  $\text{CO}_2$  by other hydroxylated adsorbents.

### Conflicts of interest

Authors have no conflicts of interest to declare.

### Acknowledgments

This work was supported by grants from MDEIE-FQRNT (2011-GZ-138312) and FODAR-UQ-2015 (QC, Canada) to AA and RR.

### References

- [1] R. Monastersky, *Nature*, 2009, **458**, 1091-1094.
- [2] A. Yamasaki, *J. Chem. Eng. Japan*, 2003, **36**, 361-375.
- [3] J. C. Abanades, E. S. Rubin, E. J. Anthony, *Ind. Eng. Chem. Res.*, 2004, **43**, 3462-3466.
- [4] S. Choi, J. H. Drese, C. W. Jones, *ChemSusChem: Chem. Sustain. Energy Mater.*, 2009, **2**, 796-854.
- [5] S. Cavenati, C. A. Grande, A. E. Rodrigues, *Chem. Eng. Sci.*, 2006, **61**, 3893-3906.
- [6] C. A. Grande, A. E. Rodrigues, *Int. J. Greenh. Gas Control*, 2008, **2**, 194-202.
- [7] J. Zhang, P. A. Webley, P. Xiao, *Energy Convers. Manag.*, 2008, **49**, 346-356.
- [8] A. Azzouz, A.-V. Ursu, D. Nistor, T. Sajin, E. Assaad, R. Roy, *Thermochim. Acta*, 2009, **496**, 45-49.
- [9] A. Azzouz, S. Nouisir, N. Platon, K. Ghomari, T. C. Shiao, G. Hersant, J.-Y. Bergeron, R. Roy, *Int. J. Greenh. Gas Control*, 2013, **17**, 140-147.
- [10] A. Azzouz, S. Nouisir, N. Platon, K. Ghomari, G. Hersant, J.-Y. Bergeron, T. C. Shiao, R. Rej, R. Roy, *Mater. Res. Bull.*, 2013, **48**, 3466-3473.
- [11] A. Azzouz, E. Assaad, A.-V. Ursu, T. Sajin, D. Nistor, R. Roy, *Appl. Clay Sci.*, 2010, **48**, 133-137.
- [12] S. Nouisir, N. Platon, K. Ghomari, A.-S. Sergentu, T. C. Shiao, G. Hersant, J.-Y. Bergeron, R. Roy, A. Azzouz, *J. Colloid Interface Sci.*, 2013, **402**, 215-222.
- [13] A. Azzouz, N. Platon, S. Nouisir, K. Ghomari, D. Nistor, T. C. Shiao, R. Roy, *Sep. Purif. Technol.*, 2013, **108**, 181-188.
- [14] J. Leclaire, Y. Coppel, A.-M. Caminade, J.-P. Majoral, *J. Am. Chem. Soc.*, 2004, **126**, 2304-2305.
- [15] C. Hawker, R. Lee, J. Fréchet, *J. Am. Chem. Soc.*, 1991, **113**, 4583-4588.
- [16] N. Bouazizi, D. Barrimo, S. Nouisir, R. Ben Slama, T. C. Shiao, R. Roy, A. Azzouz, *J. Energy Inst.*, 2018, **91**, 110-119.
- [17] A. V. Arus, M. N. Tahir, R. Sennour, T. C. Shiao, L. M. Sallam, I. D. Nistor, R. Roy, A. Azzouz, *ChemistrySelect*, 2016, **1**, 1452-1461.
- [18] A. Azzouz, S. Nouisir, N. Bouazizi, R. Roy, *ChemSusChem*, 2015, **8**, 800-803.
- [19] A. Azzouz, S. Nouisir, N. Bouazizi, R. Roy, *Technical Proceedings of the 2014 NSTI Nanotechnology Conference and Expo, NSTI-Nanotech, Washington-National Harbor*, CRC Press, Boca Ration, FL, USA, 2014, Paper number 396, 72-75 pages.
- [20] J.-C. Bergonzini, C. Duby, "Analyse et planification des expériences", in *Les dispositifs en blocs*, Masson, Paris, France, 1995.

- [21] A. Azzouz, *Concepte de modelare si elemente de strategie in design industrial*, Tehnica-Info, Chisinau, Moldova, 2002.
- [22] G. Sado, M.-C. Sado, *Les plans d'expériences: de l'expérimentation à l'assurance qualité*, AFNOR, Paris, France, 2001.
- [23] W. E. Duckworth, J. B. Le Gall, *Méthodes statistiques de la recherche technologique*, Dunod, Paris, France, 1973.